Supramolecular Recognition of Quaternary Phosphonium Cations

Mark P. Walsh, [†,¢] *Matthew O. Kitching*[†]*

[†] Department of Chemistry, Durham University, Durham, DH1 3LE, UK

[¢] School of Chemistry, University of Bristol, Bristol, BS8 1TS, UK

*Correspondence to be sent to matthew.o.kitching@durham.ac.uk

Keywords: Supramolecular recognition, BINOL, hydrogen bonding, phosphonium cations

ABSTRACT

The modes of supramolecular recognition of quaternary phosphonium cations mediated by 1,1′-bi-2-naphthol (BINOL) are identified and characterized. In contrast to our previous work on ammonium cations, the recognition of the quaternary phosphonium cations via the formation of a $PR_4^+ \cdot Br^- \cdot$BINOL ternary complex was found to be mediated by: a hydrogen bond from an α-carbon center of the phosphonium cation, encapsulation within a continuous hydrogen bond network between the halide–BINOL network, or a combination of these effects working in tandem. The solid state structures of these ternary complexes were analyzed by X-ray crystallography, aided by Hirshfeld surface analysis, to confirm the presence of characteristic intermolecular interactions for the identified modes. In all cases, the quaternary phosphonium cation acts as a

hydrogen bond donor (HBD) in these supramolecular interactions, and thus is key to the recognition process with BINOL. The characterization of such mechanisms offers insight to the supramolecular and crystal engineering communities in the future design of agents capable of the supramolecular recognition of phosphonium cations and their abstraction from the solution phase.

INTRODUCTION

Understanding the interactions between molecular entities is key to the design of new supramolecular systems. The solution phase recognition of cations has led to significant achievements in the field of supramolecular chemistry. Such recognition has been commonly achieved through hydrogen bond formation between the recognition unit and the target cation. The most commonly studied species are ammonium cations, which have been observed to undergo supramolecular recognition by crown ethers,[1–4] cyclodextrins,[5] cavitands,[6,7] cucurbiturils,[8,9] pillar[n]arenes,[10,11] and calix[n]arenes.[12–14] Generally these examples employ protonated ammonium cations where the polarized N^+–H bond allows strong hydrogen bonding in the host:guest complex (for examples, hydrogen bond donor parameter, $\alpha = 4.5$ for NEt_3HBPh_4).[15] Similarly, for the small number of examples of supramolecular recognition of phosphorus centers, phosphine oxides have garnered the most study due to the strong hydrogen bond acceptor (HBA) properties of the oxide motif (hydrogen bond acceptor parameter, $\beta = 10.7$, for $Bu_3P{=}O$).[16,17] BINOL was first identified as a means to recognize and resolve phosphine oxides by direct hydrogen bonding by Toda *et al*[18] and was recently expanded to include α,α,α′,α′-tetraaryl-2,2-disubstituted-1,3-dioxolane-4,5-dimethanol (TADDOL) and dibenzoyltartaric acid (DBTA) as competent recognition units by Bagi *et al*.[19,20] In terms of quaternary phosphonium salts, much less attention has been dedicated to its supramolecular recognition of these species. The importance of such interactions has been recently highlighted by Phipps and coworkers. [21] In their

work, Phipps *et al.* exploit an ion pairing mechanism to perform a supramolecular assembly of a phosphonium substrate and a sulfonate containing iridium catalyst to mediate a regioselective borylation. Due to our group's recent work highlighting the enantioselective recognition of quaternary ammonium cations using enantiopure BINOL via a proposed hydrogen bonding event to the α-carbon center of the ammonium cation, we sought to explore the possibility of this same behavior in quaternary phosphonium cations.[22]

Based on our previous recognition of ammonium cations, we foresaw that multiple interactions may be possible within the supramolecular recognition of a phosphonium cation. The first possibility was the formation of a continuous hydrogen bond network *via* BINOL-halogen hydrogen bonding (Figure 1, *Type A*). Such a hydrogen bond network would encapsulate the phosphonium cation, which is bound to the halogen counterion by electrostatic interactions. A second possibility is the expected hydrogen bonding from the BINOL hydroxyl to the halogen counterion, while the α-centre of the phosphonium cation also acts as a HBD to the halogen, forming the ternary complex ($PR_4^+ \cdot X^- \cdot$BINOL) (Figure 1, *Type B*). In this case, the continuous hydrogen bond network between the BINOL hosts is not strictly necessary to recognize the phosphonium cation, instead it is indirectly recognized using the halogen as a mediator species. The third case would be the hydroxyl groups on the BINOL species participating as a HDB to the halogen counterion, while also acting as a HBA for the α-centre of the phosphonium cation (Figure 1, *Type C*). In this manner, the phosphonium cation would be directly recognized by the BINOL host within the ternary complex. The final possibility would be a combination of the above effects; where the mixture of encapsulation, indirect, and direct recognition mechanisms determine how the phosphonium cation is recognized in the presence of BINOL.

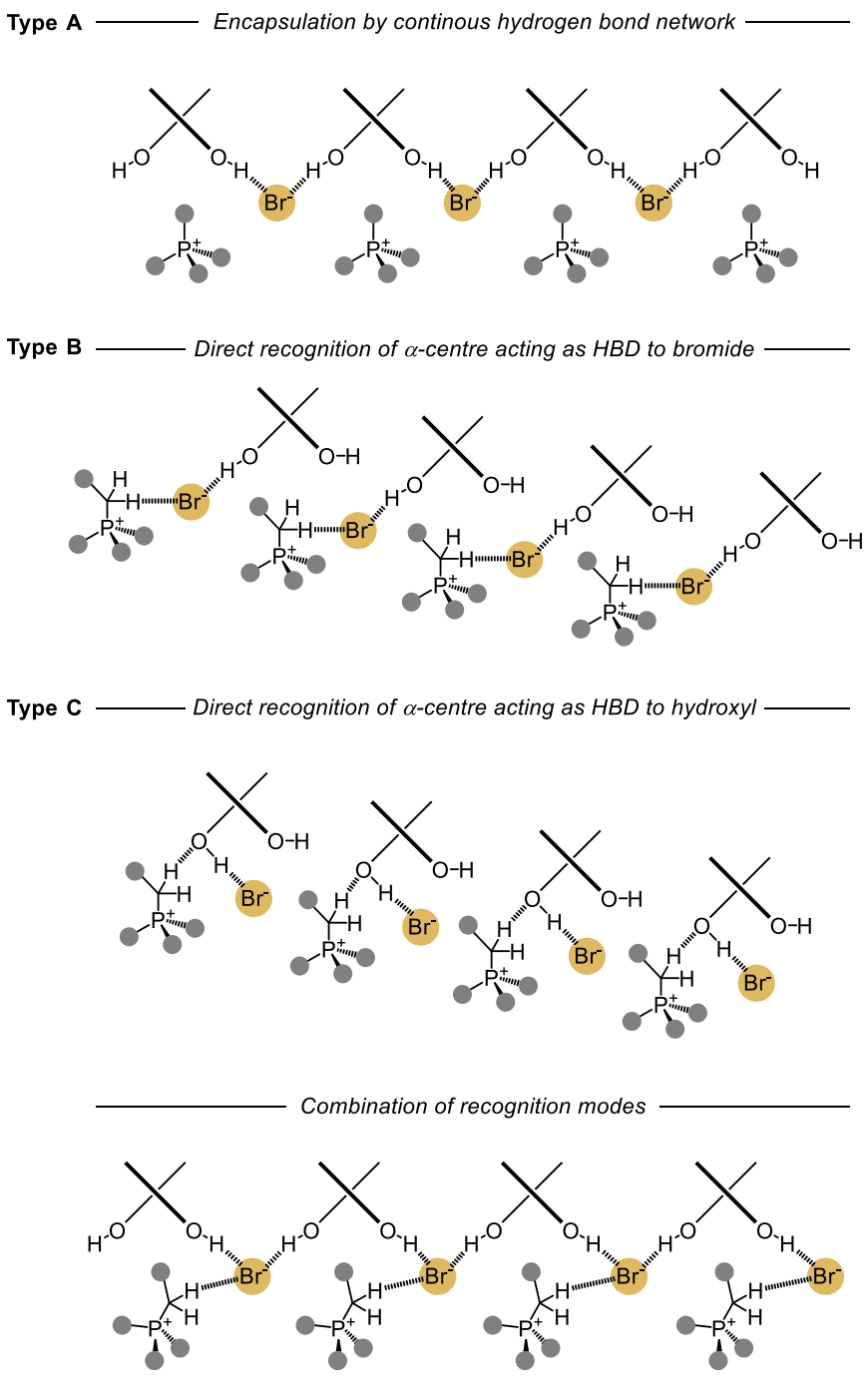

Figure 1 - Modes of supramolecular recognition

RESULTS

Synthesis. The synthesis of the quaternary phosphonium salts was achieved through simple alkylation of commonly available achiral phosphines with either allyl or benzyl bromide (see Figure 2). Alkylation of triphenylphosphine yielded **1** (R_2 = CH=CH_2, 96%) and **2** (R_2 = Ph, 91%), and alkylation of tributylphosphine yielded **3** (R_2 = CH=CH_2, 99%). Upon their synthesis and isolation, single crystals of both **1** and **2** were subsequently obtained and analyzed by X-ray crystallography (see Supplementary Information).

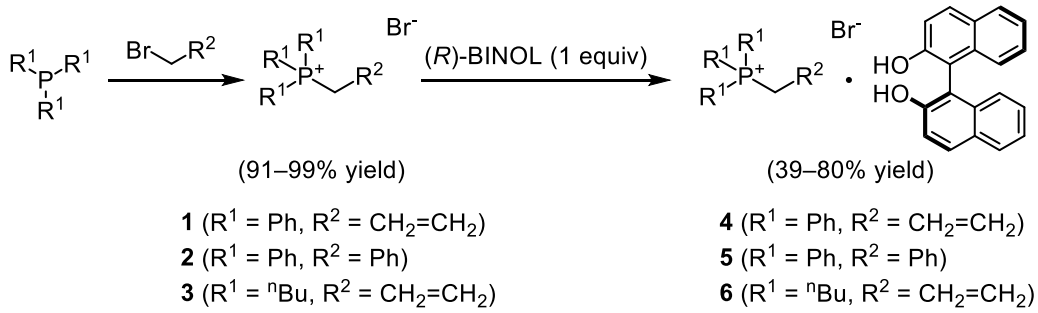

Figure 2 - Synthesis of the quaternary phosphonium salts and their respective ternary complexes with (*R*)-BINOL

Recognition. The recognition of these quaternary phosphonium salts was then attempted. In concentrated $CHCl_3$ solutions **1** and **3** formed solid ternary complexes with (*R*)-BINOL to give **4** (74%) and **6** (80%) respectively and were isolated by filtration. **2** failed to yield the desired ternary complex in $CHCl_3$, even upon concentration. When the solvent was changed to ethanol however, the complex **5** formed in lower yield (39%) compared to the previously mentioned ternary complexes. ^{1}H NMR and melting points of the isolated solids indicated transformation to the desired ternary complexes. However, only crystallographic analysis of the solid-state structure could give further information of the supramolecular recognition.

Crystallography. Single crystals of each ternary complex were grown. **4** readily crystallised in CD_3OD to give large clear prisms. Crystals of **5** and **6** were grown by gradual cooling and

evaporation in ethanol to give large clear prisms and plates respectively. Acquisition of the single crystal diffraction data for each sample gave unambiguous evidence for the formation of the ternary complexes in the solid state. The X-ray crystallographic data for each ternary complex is given in Table 1.

In the crystal structure of complex **4**, there is clear hydrogen bonding between the phenolic hydroxyl group of the BINOL and the Br^- counterion (O–H···Br^-; d = 2.349 Å, θ = 174.11°). In addition, another hydrogen bond is also present from the α-carbon center of the phosphonium salt to the bromide counterion (C–H···Br^-; d = 2.826 Å, θ = 162.72°). Such interactions are consistent with supramolecular ternary complex formation between the BINOL, halide and the target phosphonium cation. Interestingly, unlike the previous examples in quaternary ammonium complexation, no continuous hydrogen bonding network between the BINOL and bromide counterions appears to be present, with each BINOL bound to only a single bromide anion (as displayed in Figure 3 a). For this reason, complex **4** is designated a *Type B* recognition, where there is no continuous BINOL···halogen network and the phosphonium is acting as a HBD to the halogen counterion via an acidic α-centre of the phosphonium cation. Minor aryl C–H···O interactions (d = 2.693 Å, θ = 120.68°; d = 2.622, θ = 124.05° & d = 2.630 Å, θ = 142.10°) from the electronically deficient phenyl rings of the phosphonium cation to the hydroxyl groups of the BINOL are present.[23] These minor interactions were not classed as forms of recognition (see *Hirshfeld Surface Analysis*, below), however, their presence in the crystal structure should not be discounted as the full intricacies of this phenomenon is not fully understood.

The crystal structure of complex **5** presented also contained strong interactions between the BINOL and bromide counterion. A strong hydrogen bond between the bromide counterion and BINOL was immediately evident (O–H···Br^-; d = 2.442 Å, θ = 177.77°). However, in contrast to

complex **4**, the packing in this crystal structure revealed a continuous hydrogen bonding network linking each BINOL moiety to two adjacent bromide anions (see Figure 3 b). A hydrogen bond from the acidic α-carbon center of the phosphonium cation is also observed (C–H···Br^-; d = 2.652 Å, θ = 172.00°), allowing for the formation of the ternary complex. There is also a noteworthy aryl C–H···O hydrogen bond (d = 2.409 Å, θ = 164.81°), from the phenyl ring of the phosphonium to an adjacent hydroxyl group of the BINOL species. In this way, it is shown that the recognition of this phosphonium salt is mediated by all three types of hypothesized recognition modes: a *Type A* encapsulation mechanism (*via* the continuous BINOL-halogen hydrogen bond network), a *Type B* indirect recognition of the α-center of the phosphonium cation acting as a HBD to the halogen counterion and a *Type C* direct recognition via aryl C–H···O hydrogen bonding to the hydroxyl HBA on the BINOL species. This demonstrates that that an acidic α-centre on the phosphonium is not the only possible HBD motif in this recognition process and that electron deficient aryl rings are also sufficient for hydrogen bonding to the BINOL species. It also highlights the variety in recognition modes that can be responsible for the formation of one ternary complex.

Analysis of complex **6** revealed the expected hydrogen bonding between the BINOL and bromide counterion (O–H···Br^-; d = 2.349 Å, θ = 174.11°) (see Figure 3 c). This crystal structure also had a continuous hydrogen bonding network between the BINOL and bromide counterions, which appear to encapsulate the phosphonium cation, consistent with a *Type A* recognition. However, no close contacts between the phosphonium cation and the bromide counterion could be classed as hydrogen bonding. Instead, C–H···O hydrogen bonds (C–H···O; d = 2.517 Å, θ = 161.39°, d = 2.575 Å, θ = 126.28°) from the α-carbon centre of the phosphonium cation acting as the HBD and the BINOL hydroxyl group acting as a HBA were present. This demonstrates that both *Type A* and *Type C* modes of recognition are responsible for complex formation.

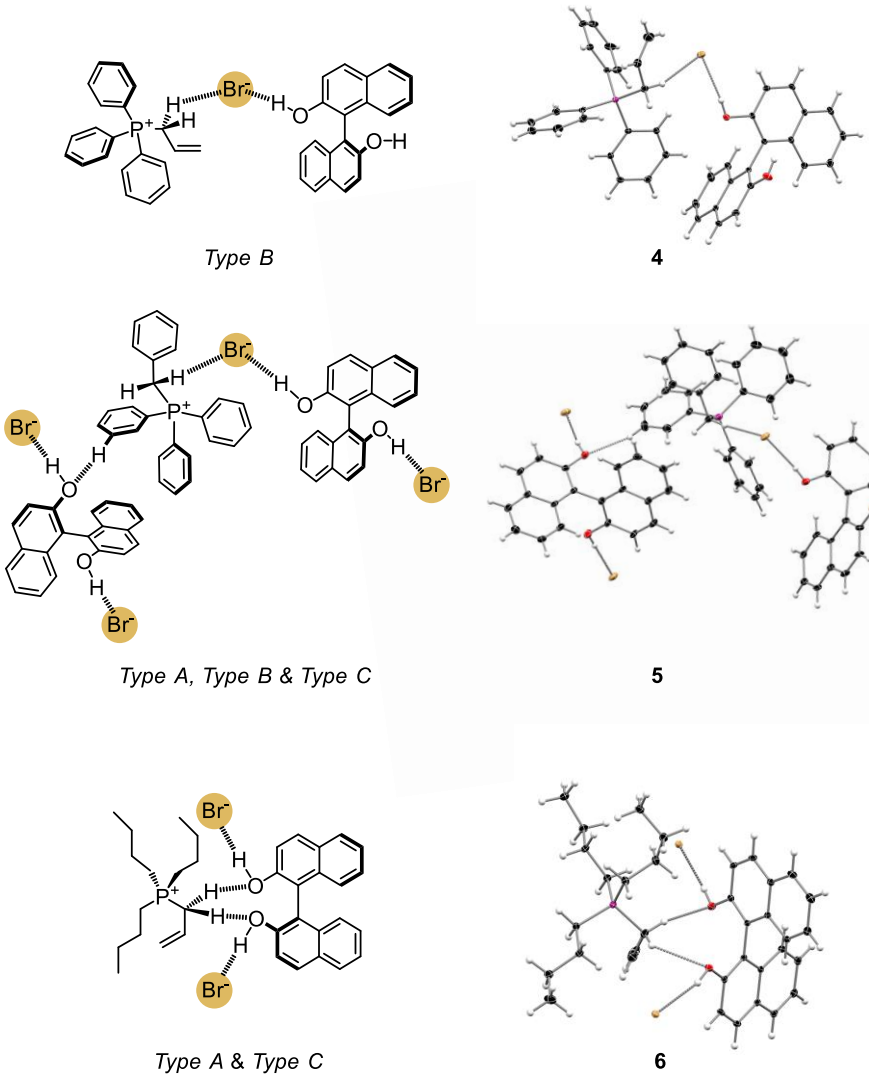

Figure 3 – Supramolecular interactions identified in the solid state by X-ray crystallography

166 Table 1 – Crystallographic data for the ternary complexes

	4	**5**	**6**
Empirical formula	$C_{41}H_{34}BrO_2P$	$C_{45}H_{36}BrO_2P$	$C_{35}H_{46}BrO_2P$
Formula weight	669.56	719.62	609.60
Temperature/K	120.0	120.0	120.0
Crystal system	monoclinic	monoclinic	orthorhombic
Space group	$P2_1$	$P2_1$	$P2_12_12_1$
a/Å	10.9509(5)	8.8952(15)	12.5247(5)
b/Å	14.5495(7)	15.823(3)	15.2027(6)
c/Å	11.0440(6)	12.673(2)	16.4528(7)
α/°	90	90	90
β/°	113.207(2)	96.325(7)	90
γ/°	90	90	90
Volume/Å^3	1617.26(14)	1772.9(5)	3132.8(2)
Z	2	2	4
ρ_{calc}g/cm^3	1.375	1.348	1.292
μ/mm^{-1}	1.356	1.243	1.393
F(000)	692.0	744.0	1288.0
Crystal size/mm^3	0.273 × 0.266 × 0.162	0.281 × 0.222 × 0.096	0.276 × 0.234 × 0.216
Radiation	MoKα (λ = 0.71073)	MoKα (λ = 0.71073)	MoKα (λ = 0.71073)
2Θ range for data collection/°	4.012 to 63.166	4.608 to 54.158	4.088 to 64.27
Index ranges	-16 ≤ h ≤ 16, -21 ≤ k ≤ 21, -16 ≤ l ≤ 16	-11 ≤ h ≤ 11, -20 ≤ k ≤ 20, -16 ≤ l ≤ 16	-18 ≤ h ≤ 18, -22 ≤ k ≤ 22, -24 ≤ l ≤ 24
Reflections collected	37669	30239	77675
Independent reflections	10748 [R_{int} = 0.0555, R_{sigma} = 0.0726]	7774 [R_{int} = 0.1175, R_{sigma} = 0.1416]	10995 [R_{int} = 0.0744, R_{sigma} = 0.0625]
Data/restraints/parameters	10748/1/408	7774/1/444	10995/0/403
Goodness-of-fit on F^2	0.993	0.930	0.985
Final R indexes [I>=2σ (I)]	R_1 = 0.0352, wR_2 = 0.0711	R_1 = 0.0524, wR_2 = 0.1029	R_1 = 0.0323, wR_2 = 0.0618
Final R indexes [all data]	R_1 = 0.0490, wR_2 = 0.0740	R_1 = 0.0968, wR_2 = 0.1174	R_1 = 0.0489, wR_2 = 0.0655
Largest diff. peak/hole / e Å^{-3}	0.52/-0.49	0.51/-0.85	0.45/-0.38
Flack parameter	0.041(4)	0.012(9)	0.016(3)

167

Hirshfeld Surface analysis. Further characterization of the recognition modes within the crystal structures was achieved using Hirshfeld surface analysis (Figure 4).[24] Highlighting the C–H···Br^- interactions in each plot qualitatively displays the presence and strength of this interaction in each crystal structure (blue traces). In complexes **4** and **5** (Figure 4 a & b) a sharp characteristic fingerprint is revealed indicative of a hydrogen bond present in these crystals, further confirming the observation of both crystals having a *Type B* component in their recognition modes. Complex **6** however, has a much weaker and more diffuse fingerprint for this interaction (Figure 4 c). While this interaction is present in the crystal, it is unlikely to be a defined hydrogen bond as its overall contribution to the entire crystal packing is minimal representing just 2.6% of the surface area of the plot. This is likely indicative to the fact that this crystal has been identified to have both *Type A* and *Type C* recognition, which does not involve strong C–H···Br^- interactions.

The C–H···O interactions with the hydroxyl group of the BINOL acting as a HBA could also be clearly examined (purple traces). In complex **4**, noticeably more diffuse, and therefore weaker, C–H···O interactions are present, consistent with the absence of *Type C* direct recognition. Instead the plot for complex **4** is dominated by the C–H···Br^- interactions indicative of *Type B* recognition. In complex **5**, equally sharp traces for C–H···Br^-, and C–H···O interactions are visible, confirming the present of both *Type B* and *Type C* recognition modes in this ternary complex. Finally, the Hirshfeld plot for complex **6** displays the overwhelming contribution of the C–H···O hydrogen bonding observed in this crystal (5.8% of the plot), showing strong evidence for a *Type C* recognition in this complex, with little to no *Type B* character.

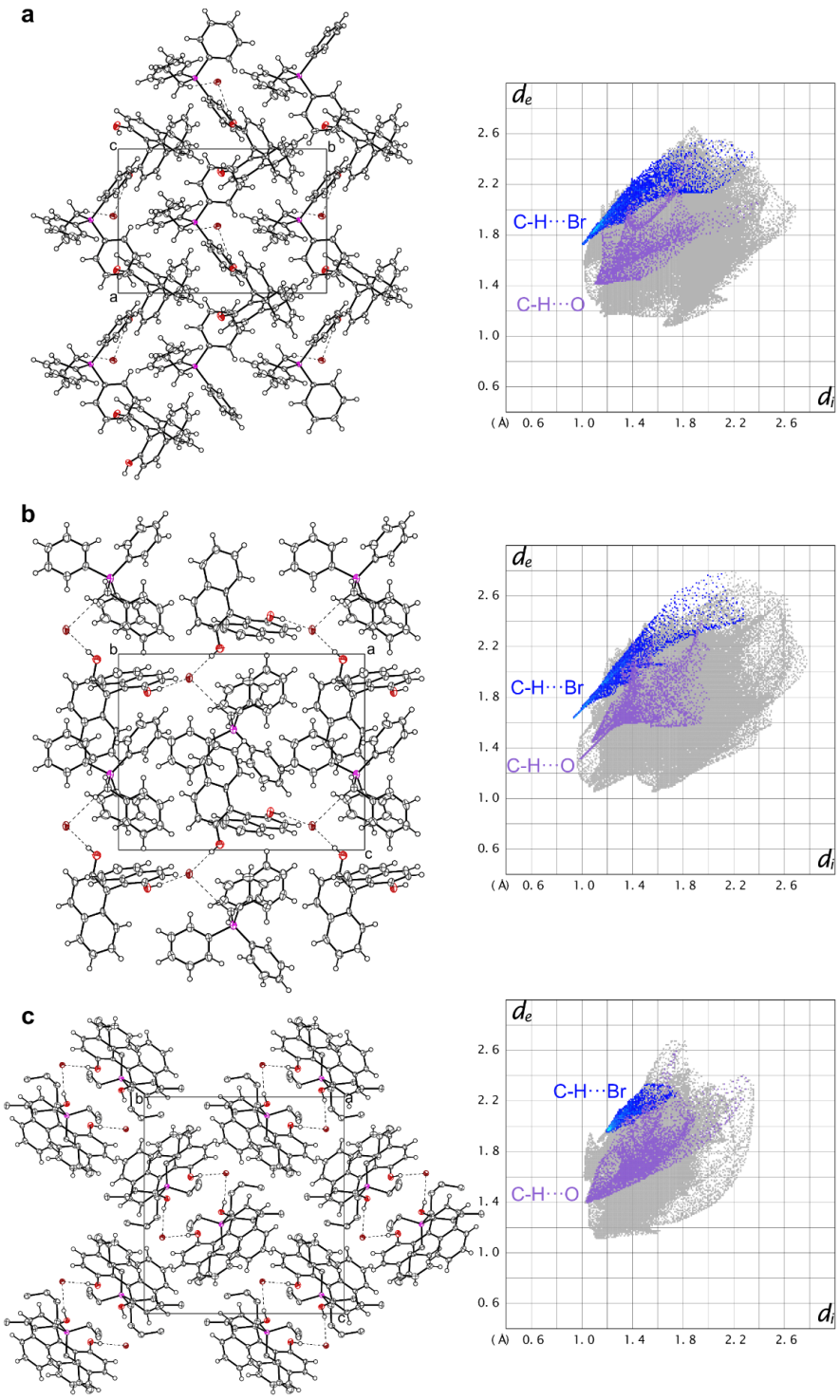

Figure 4 – Expanded unit cells and Hirshfeld fingerprint plots for (a) complex **4**, (b) complex **5**, and (c) complex **6**; highlighting the P^+–CH···Br^- interactions (blue) and P^+–CH···O (purple) observed in each ternary complex

188

BINOL···X⁻ packing. To view the impact of the different modes of recognition on the packing of each complex, both the bromide and BINOL species are represented as their Van der Waals surface. The phosphonium cations could then be more easily viewed within the architecture of the BINOL···Br⁻ scaffold (Figure 5). Complex **4**, which displays *Type B* recognition, can be seen in Figure 5 a. In this rendering, the non-continuous BINOL network is apparent. Instead, the packing is much closer to a standard co-crystallization between the BINOL and the phosphonium salt where the halide counter-ion is more accessible to the phosphonium cation.

Complexes **5** (Figure 5 b) and **6** (Figure 5 c) both show much more compact packing structure around the phosphonium cation – indicative of a *Type A* recognition – in which the cation is encapsulated within a continuous BINOL···Br⁻ hydrogen bond network. The phosphonium cation is accommodated in visible cavities within this hydrogen bond network. Interestingly, this is despite the differences in geometry between the respective phosphonium cations within the two crystal structures. This demonstrates that the encapsulation of the cation is a flexible process – rather than the BINOL only able to accommodate one specific shape, the cavities found within these crystal structures are not of a fixed volume or geometry.

We speculate that initial recognition of the phosphonium cation in complexes **5** and **6** involves either indirect (*via* the halogen counterion, *Type B*) or direct (*Type C*) hydrogen bond interactions between a BINOL species and the phosphonium cation in solution. The BINOL then propagates the growth of the complex through a second hydrogen bond to an adjacent halogen counterion, thus 'recruiting' a second phosphonium cation. These supramolecular interactions greatly increase the rate of nucleation until a critical mass is reached, when the whole recognition network has greatly reduced solubility and the complex is pulled from solution as a microcrystalline solid.

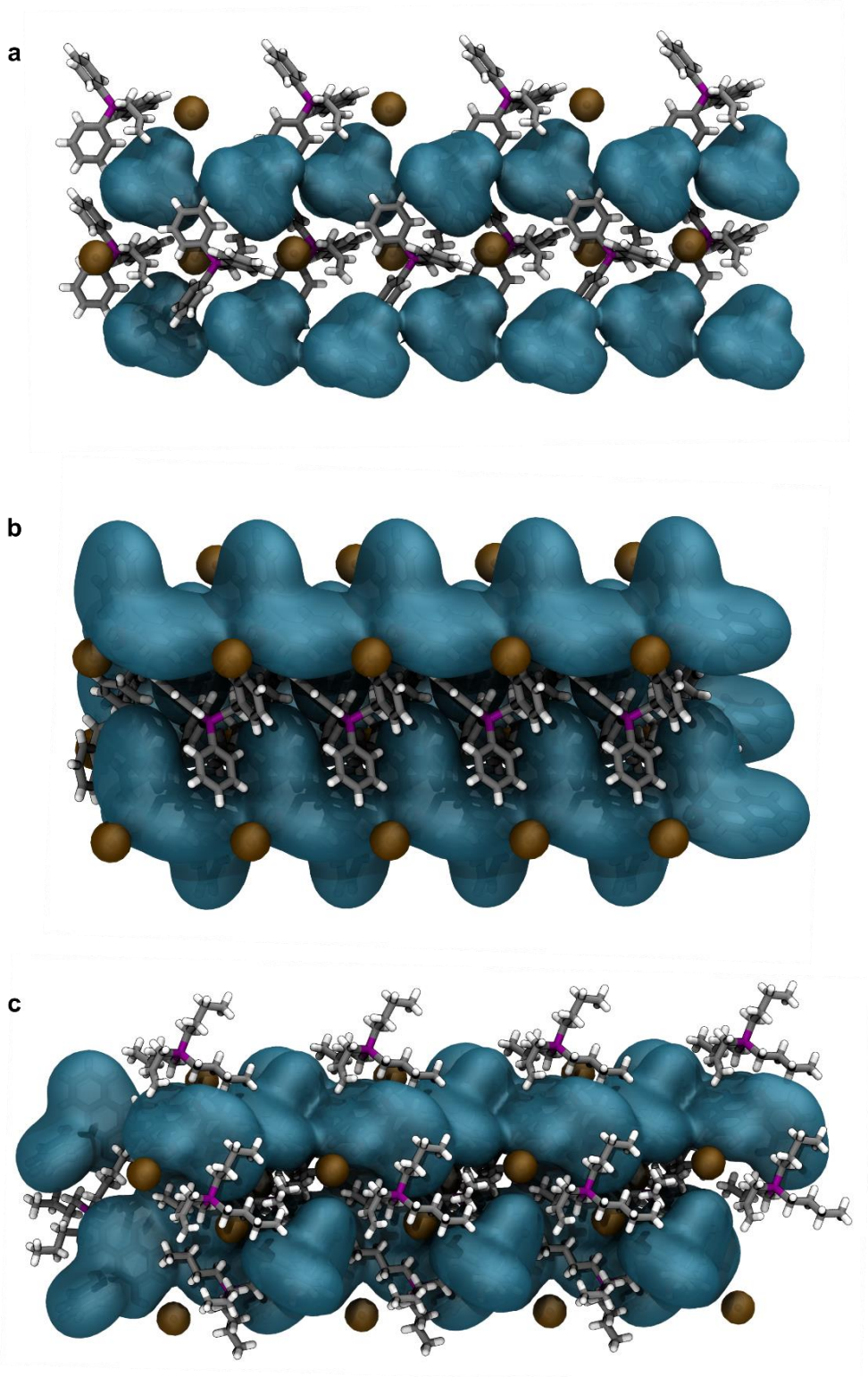

Figure 5 – The resulting packing in the crystal structures of the recognition complexes, where (a) is complex **4**, (b) is complex **5**, and (c) is complex **6**. The van der Waals radii for each BINOL (teal) and bromide (brown) species is shown, with the phosphonium cations represented as stick representations within the crystal structure

211

CONCLUSION

This work characterizes the modes of supramolecular recognition of quaternary phosphonium cations in the solid phase by BINOL. Three modes have been hypothesized and subsequently identified within the recognition complexes presented here. Complex **4** arises from *Type B* interactions, while complex **5** has a mixture of *Type A, Type B* and *Type C* character as identified by single crystal X-ray crystal structure and Hirshfeld fingerprint plots. Complex **6** contains *Type A & C* recognition motifs in its solid state structure. The crystal packing of each recognition complex was influenced by these modes of interaction and presents new crystal engineering opportunities in the co-crystallisation of BINOL with ionic species.

EXPERIMENTAL

Reagents and solvents used in this work were commercially available (*Sigma Aldrich*; tributylphosphine, triphenylphosphine. *Fluorochem*; (*R*)-BINOL, allyl bromide, benzyl bromide) and were used without further purification. NMR spectra were recorded on either a *Bruker* Avance III HD-400 spectrometer with operating frequencies of 400.07 MHz for ^{1}H; 100.60 MHz for ^{13}C and; 161.95 MHz for ^{31}P at 298 K. Melting points are uncorrected. X-ray single crystal diffraction data was collected using a *Bruker* D8 Venture (Photon100 CMOS detector, ImSmicrosource, focusing mirrors). The diffractometer was equipped with an *Oxford Cryosystems* cryostream, with open-flow nitrogen cryostats set at a temperature of 120.0 K. All structures were solved by direct methods and refined by full-matrix least squares on F2 for all data using Olex2 (V 13.0)[25] and SHELXTL[26,27] software. All non-disordered non-hydrogen atoms were refined anisotropically and hydrogen atoms were placed in the calculated positions and refined in riding mode. Crystallographic data and related CIFs for the structures related to the submitted publication have

been deposited with the *Cambridge Crystallographic Data Centre* as supplementary publications: CCDC 2048561–2048565. Hirshfeld surfaces and fingerprint plots were generated using *Crystal Explorer* (V 17.5)[24] and full unedited fingerprint plots are available in the Supplementary Information. Full descriptions for the synthesis of all compounds and characterization data are described in the Supplementary Information.

Typical alkylation procedure. *Synthesis of Allyltributylphosphonium bromide* (**3**).

To a neat solution of tributylphosphine (2.47 mL, 10.0 mmol) was added allyl bromide (0.95 mL, 11.0 mmol) dropwise over 15 mins with stirring. Caution: the reaction is highly exothermic. The solution was allowed to react at room temperature for 30 minutes. The viscous reaction mixture cooled upon completion of the alkylation and crystallised as a colourless solid. The solid was washed with diethyl ether (3 x 15 mL) and dried in vacuo to afford 3 as a colourless white solid (3.18 g, 99% yield).

^{1}H NMR (400 MHz, $CDCl_3$) δ 5.80 – 5.60 (m, 1H), 5.49 (ddd, J = 16.8, 3.8, 1.0 Hz, 1H), 5.38 (ddd, J = 10.0, 4.4, 1.1 Hz, 1H), 3.49 (dd, J = 15.7, 7.5 Hz, 2H), 2.52 – 2.29 (m, 6H), 1.76 – 1.24 (m, 12H), 0.90 (q, J = 7.1 Hz, 9H). ^{13}C NMR (101 MHz, $CDCl_3$) δ 124.3 (d, J = 11.7 Hz), 124.0 (d, J = 9.9 Hz), 25.1 (d, J = 47.0 Hz), 23.8 (d, J = 15.3 Hz), 23.6 (d, J = 4.9 Hz), 18.8 (d, J = 47.0 Hz), 13.3. ^{31}P NMR (202 MHz, $CDCl_3$) δ 31.32. HRMS (ESI-TOF) m/z: $[M]^+$ Calculated for $C_{15}H_{23}P^+$: 243.2242, found 243.2269. mp: 47–50 °C. IR (max/cm^{-1}): 2961s, 2871s, 1634m, 1464m, 1232m, 1093m, 929m, 719m, 597m.

Typical complexation procedure. *Allyltributylphosphonium bromide · (R)-1,1'-bi-2-naphthol* (**6**).

The quaternary phosphonium bromide salt **3** (0.969 g, 3.00 mmol) was dissolved in $CHCl_3$ (1.5 mL, 2.0 M) in a 10 mL vial. Solid (*R*)-BINOL (0.858 g, 1.0 equiv) was then added with stirring to the solution, resulting in a pale-yellow homogeneous solution. This solution was allowed to stir at room temperature overnight, which produced the desired complexed product **6** as a white precipitate. The resulting solid complex was isolated by vacuum filtration (1.47 g, 80% yield). ^{1}H NMR (400 MHz, DMSO-d_6) δ 9.26 (s, 2H), 7.96 – 7.74 (m, 4H), 7.39 (d, *J* = 8.8 Hz, 2H), 7.22 (ddd, *J* = 8.1, 6.7, 1.3 Hz, 2H), 7.16 (ddd, *J* = 8.3, 6.7, 1.4 Hz, 2H), 6.96 (dd, *J* = 8.4, 1.2 Hz, 2H), 5.81 (dddd, *J* = 17.4, 10.0, 7.5, 4.8 Hz, 1H), 5.51 – 5.39 (m, 1H), 5.35 (ddd, *J* = 10.0, 12 4.0, 1.6 Hz, 1H), 3.26 (dd, *J* = 14.7, 7.3 Hz, 2H), 2.33 – 2.13 (m, 6H), 1.49 (tdd, *J* = 10.9, 8.2, 5.8 Hz, 6H), 1.39 (h, *J* = 7.0 Hz, 6H), 0.90 (t, *J* = 7.2 Hz, 9H). ^{13}C NMR (101 MHz, DMSO-d_6) δ 153.0, 134.1, 128.5, 128.1, 127.8, 125.7, 125.5 (d, *J* = 9.4 Hz), 124.4, 123.0 (d, *J* = 11.9 Hz), 122.2, 118.5, 115.4, 23.8, 23.3 (d, *J* = 15.7 Hz), 22.6 (d, *J* = 4.5 Hz), 17.4 (d, *J* = 47.2 Hz), 13.2. ^{31}P NMR (202 MHz, DMSO-d_6) δ 32.18. HRMS (ESI-TOF) m/z: $[M]^+$ calculated $C_{15}H_{32}P^+$: 243.2242, found 243.2263. $[M\text{-}H]^-$ calculated $C_{20}H_{13}O_2^-$: 285.0921, found 285.0929. mp: 140–141 °C (MeOH). IR (max/cm^{-1}): 3165br, 2954m, 1622m, 1504m, 1324m, 1269s, 964m, 818s, 683m. XRD: Sample was crystallised in ethanol, to give clear colorless prisms. Crystal data: orthorhombic, space group $P2_12_12_1$ (no. 19).

ASSOCIATED CONTENT

Supporting Information. A listing of the contents of each file supplied as Supporting Information should be included. For instructions on what should be included in the Supporting Information as well as how to prepare this material for publications, refer to the journal's Instructions for Authors. The following files are available free of charge. Supporting Information (PDF) Crystallographic files (CIF)

AUTHOR INFORMATION

Corresponding Author

Matthew O. Kitching, email: matthew.o.kitching@durham.ac.uk

Present Addresses

† Department of Chemistry, Durham University, Stockton Road, DH1 3LE, UK

¢ School of Chemistry, University of Bristol, Bristol, BS8 1TS, UK

Author Contributions

The manuscript was written by M.O.K. and M.P.W. All authors have given approval to the final version of the manuscript. Experimental work and crystallographic analysis was conducted by M.P.W.

Funding Sources

M.O.K. acknowledges funding from the Royal Society in the form of a University Research Fellowship (UF150536) and equipment grant (RGS\R2\180467)**.** Durham University is acknowledged for providing a doctoral studentship (M.P.W.)

ABBREVIATIONS

HBD – hydrogen bond donor, HBA – hydrogen bond acceptor, BINOL - 1,1′-bi-2-naphthol, d – interatomic distance, θ – bond angle

REFERENCES

(1) Kyba, E. B.; Koga, K.; Sousa, L. R.; Siegel, M. G.; Cram, D. J. Chiral Recognition in Molecular Complexing. *J. Am. Chem. Soc.* **1973**, *95* (8), 2692–2693.

(2) Cheng, M.; Liu, X.; Luo, Q.; Duan, X.; Pei, C. Cocrystals of Ammonium Perchlorate with a Series of Crown Ethers: Preparation, Structures, and Properties. *Cryst. Eng. Comm.* **2016**, *18* (8487–8496).

(3) Cram, D. J. The Design of Molecular Hosts, Guests, and Their Complexes. *Angew. Chem. Int. Ed.* **1988**, *27* (8), 1009–1112.

(4) Kyba, E. P.; Helgeson, R. C.; Madan, K.; George W. Gokel; Tarnowski, T. L.; Moore, S. S.; Cram, D. J. Host-Guest Complexation. 1. Concept and Illustration. *J. Am. Chem. Soc.* **1977**, *99* (8), 2564–2571.

(5) Datta, B.; Roy, A.; Roy, M. N. Inclusion Complexation of Tetrabutylammonium Iodide by Cyclodextrins. *J. Chem. Sci.* **2017**, *129* (5), 579–587.

(6) Moran, J. R.; Karbach, S.; Cram, D. J. Cavitands: Synthetic Molecular Vessels. *J. Am. Chem. Soc.* **1982**, *104*, 5826–5828.

(7) Freeman, W. A. Structures of the P-Xylylenediammonium Chloride and Calcium Hydrogensulfate of the Cavitand “Cucurbituril”, C36H36N24O12. *Acta Cryst.* **1984**, *B40*, 382–387.

(8) Freeman, W. A.; Mock, W. L.; Shih, N. Y. Cucurbituril. *J. Am. Chem. Soc.* **1981**, *103* (24), 7367–7368.

(9) Márquez, C.; Hudgins, R. R.; Nau, W. M. Mechanism of Host−Guest Complexation by Cucurbituril. *J. Am. Chem. Soc.* **2004**, *126* (18), 5806–5816.

(10) Ogoshi, T.; Kanai, S.; Fujinami, S.; Yamagishi, T.; Nakamoto, Y. Para-Bridged Symmetrical Pillar[5]Arenes: Their Lewis Acid Catalyzed Synthesis and Host–Guest Property. *J. Am. Chem. Soc.* **2008**, *130*, 5022–5023.

(11) Ogoshi, T.; Yamagishi, T.; Nakamoto, Y. Pillar-Shaped Macrocyclic Hosts Pillar[n]Arenes: New Key Players for Supramolecular Chemistry. *Chem. Rev.* **2016**, *116*, 7937–8002.

(12) Shinkai, S. Calixarenes - The Third Generation of Supramolecules. *Tetrahedron* **1993**, *49* (40), 8933–8968.

(13) Lehn, J.-M.; Meric, R.; Vigneron, J.-P.; Cesario, M.; Guilhem, J.; Pascard, C.; Asfari, Z.; Vicens, J. Binding of Acetylcholine and Other Quaternary Ammonium Cations by Sulfonated Calixarenes. Crystal Structure of a [Choline-Tetrasulfonated Calix[4]Arene] Complex. *Supramol. Chem.* **1995**, *5* (2), 97–103.

(14) Beer, P. D.; Chen, Z.; Michael, G. B.; Gale, P. A. Metal, Ammonium and Alkyl Ammonium Cation Recognition by a Novel Calix[4]Arenediquinone Crown Ether. *J. Chem. Soc., Chem. Commun.* **1994**, *19*, 2207–2208.

(15) Pike, S. J.; Lavagnini, E.; Varley, L. M.; Cook, J. L.; Hunter, C. A. H-Bond Donor Parameters for Cations. *Chem. Sci.* **2019**, *10* (23), 5943–5951. https://doi.org/10.1039/c9sc00721k.

(16) Pike, S. J.; Hutchinson, J. J.; Hunter, C. A. H-Bond Acceptor Parameters for Anions. *J. Am. Chem. Soc.* **2017**, *139* (19), 6700–6706.

(17) McKenzie, J.; Feeder, N.; Hunter, C. A. H-Bond Competition Experiments in Solution and the Solid State. *CrystEngComm* **2016**, *18* (3), 394–397.

(18) Toda, F.; Mori, K.; Stein, Z.; Goldberg, I. Optical Resolution of Phosphinates and Phosphine Oxides by Complex Formation with Optically Active 2,2'-Dihydroxy-l,l'-Binaphthyl and Crystallographic Study of Two Diastereomeric Complexes with (CH3)(C6H5)(OCH3)PO. *J. Org. Chem.* **1988**, *53* (2), 308–312.

(19) Varga, B.; Herbay, R.; Székely, G.; Holczbauer, T.; Madarász, J.; Mátravölgyi, B.; Fogassy, E.; Keglevich, G.; Bagi, P. Scalable Enantiomeric Separation of Dialkyl-Arylphosphine Oxides Based on Host–Guest Complexation with TADDOL-Derivatives, and Their Recovery. *Eur. J. Org. Chem.* **2020**, 1840–1852.

(20) Varga, B.; Bagi, P. Preparation of Enantiomerically Enriched P -Stereogenic Dialkyl-Arylphosphine Oxides via Coordination Mediated Optical Resolution. *Symmetry (Basel).* **2020**, *12* (2), 215–228.

(21) Lee, B.; Mihai, M. T.; Stojalnikova, V.; Phipps, R. J. Ion-Pair-Directed Borylation of Aromatic Phosphonium Salts. *J. Org. Chem.* **2019**, *84* (20), 13124–13134.

(22) Walsh, M. P.; Phelps, J. M.; Lennon, M. E.; Yufit, D. S.; Kitching, M. O. Enantioselective Synthesis of Ammonium Cations. *Nature* **2021**, *accepted*.

(23) Bryantsev, V. S.; Hay, B. P. Influence of Substituents on the Strength of Aryl C-H···anion Hydrogen Bonds. *Org. Lett.* **2005**, *7* (22), 5031–5034.

(24) Spackman, M. A.; Jayatilaka, D. Hirshfield Surface Analysis. *Cryst. Eng. Comm.* **2009**, *11*, 19–32.

(25) Dolomanov, O. V; Bourhis, L. J.; Howard, J. A.; Puschmann, H. OLEX2: A Complete Structure Solution, Refinement and Analysis Program. *J. Appl. Cryst.* **2009**, *42*, 339–341.

(26) Sheldrick, G. M. SHELXT - Integrated Space-Group and Crystal-Structure Determination. *Acta Cryst.* **2015**, *A71*, 3–8.

(27) Hübschle, C. B.; Sheldrick, G. M.; Dittrich, B. ShelXle: A Qt Graphical User Interface for SHELXL. *J. Appl. Cryst.* **2011**, *44*, 1281–1284.

GRAPHICAL ABSTRACT